Regional Studies in Marine Science 70 (2024) 103374

Contents lists available at ScienceDirect

Regional Studies in Marine Science

journal homepage: www.elsevier.com/locate/rsma

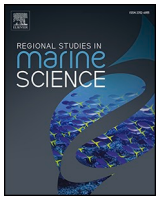

Temporal change of potential toxic element contamination, ecological and toxicological risk in holocene in Southern Black Sea coasts (Türkiye)

Ebru Yeşim Özkan [a,*], Serkan Kükrer [b], Şakir Fural [c]

[a] İzmir Katip Çelebi University, Faculty of Fisheries,Department of Marine Biology, Türkiye
[b] İzmir Katip Çelebi University, Faculty of Naval Architecture and Maritime, Department of Shipbuilding and Ocean Engineering,Türkiye
[c] Kırşehir Ahi Evran University, Faculty of Arts and Sciences, Department of Geography, Türkiye

ARTICLE INFO

Keywords:
Paleo-environmental conditions
Paleo-ecological risk
Age determination
Southern Black Sea coast

ABSTRACT

This study was carried out to evaluate the temporal variation of the potential toxic element concentration and ecological risk level during the Holocene along the Southern Black Sea coasts. Ecological and ecotoxicological indices such as enrichment factor (EF), modified ecological risk index (mRI), modified potential ecological risk index (mPER) and toxic risk index (TRI) were used in the study. Anthropogenic effects were determined to be more dominant in the western and middle parts of the Southern Black Sea Region. As, Cu, Pb, Zn, Cd, Hg, Ni enrichments were observed in the last 200 – 300 years and the potential risk index values related to them increased. Source of enrichment detected in the cores was found to be related to the volcanic activities that occurred in different geological periods. It was determined that the increases in PTE concentration observed specifically in the middle parts of the cores coincided with the dates of the volcanic activities observed in Anatolia.

1. Introduction

Recent research on the distribution and storage properties of potentially toxic elements (PTEs) in marine ecosystems has shown that contamination occurs even in deep-sea sediments. Studies have pointed out that these pollutants have more impact than expected in aquatic ecosystems (Sanei et al., 2021; Xie et al., 2022). PTEs contribute to the marine environment through natural resources, deposition, erosion, industrial pollutants, agricultural activities, untreated sewage discharge and they cause deterioration in water and sediment quality while negatively affecting human health through the food chain by reducing the quality of food products (Surricchio et al., 2019; Özkan et al., 2022; Kükrer et al., 2020; Fural et al., 2022; Peng et al., 2022). PTEs cannot be purified in biological treatment systems, and they can be released back into the water with the formation of some suitable environmental conditions, acting as a secondary source in terms of ecological and toxic risk (Järup, 2003; Rai, 2008; Varol et al., 2022).

PTEs cause significant ecological risk problems in open seas as well as inland seas with more limited wave and current systems (Nour et al., 2019; Ergin, 2020; Jeddi et al., 2021). Therefore, PTEs and other variables such as organic matter that are discharged into the inland marine ecosystem are stored at central points where the wave-current system is weak. It is known that 50% of organic waste discharged from land to sea accumulates at the margin of the continental shelf (Yanagi, 1990).

Covering an area of 436.402 km^2, the Black Sea is one of the largest inland seas in the world. The Black Sea has no connection with the open seas except for the Bosporus and Dardanelles Straits. The Black Sea, which drains a basin of approximately 2.200.000 km^2 in Europe and Asia is under anthropogenic pressure from hundreds of cities, including 22 states, 13 capitals, and a population of approximately 200.000.000 (Alkan et al., 2008). Ecological and toxicological risks likely to arise in the Black Sea may affect humans through the food chain (Makedonski et al., 2017) because fishing and seafood farming are carried out intensively in the area (Goulding et al., 2014; Balık, 2019).

The northern basin of the Black Sea, which covers an area of 1.920.000 km^2, is formed by the catchment areas of the Danube, Dniester, Dnieper, Don and Kuban Rivers (Fig. 1). Rivers in the northern basin discharge Europe's domestic and industrial waste load into the Black Sea. Rivers in the northern basin discharge Europe's domestic and industrial waste load into the Black Sea (Vera et al., 2020; Jitar et al., 2015). The southern basin of the Black Sea, on the other hand, covers an area of 280.000 km^2 and includes Türkiye's important cities, industrial facilities, agricultural areas and transportation networks. The most important rivers of the southern basin are Sakarya, Kızılırmak,

* Corresponding author.
E-mail address: ebruyesim.ozkan@ikc.edu.tr (E.Y. Özkan).

https://doi.org/10.1016/j.rsma.2024.103374
Received 16 June 2023; Received in revised form 28 December 2023; Accepted 6 January 2024
Available online 13 January 2024

Yeşilırmak and Çoruh Rivers. Recent studies conducted on a regional scale in the southern basin of the Black Sea have shown that streams discharge anthropogenic sourced PTE into the Black Sea, causing ecological risk problems at various levels (Ustaoğlu and Tepe, 2019; Ustaoğlu and Islam, 2020; Bilhan and İlalan, 2021; Yüksel et al., 2022; Yücesoy and Ergin, 1992; Bakan and Büyükgüngör, 2000; Topçuoğlu et al., 2003; Bakan and Özkoç, 2007; Balkıs et al., 2007; Ergül et al., 2008; Bat et al., 2014; Bat and Özkan, 2019; Elderwish et al., 2019; Özkoç and Arıman, 2022; Özşeker et al., 2022; Kalkan, 2022). The aforementioned studies point to ecological risk problems at various levels in the Black Sea. However, these studies reflect ecological risk problems in small parts of the Black Sea. This study aimed to; i) analyze the temporal variation of ecological and toxicological risk issues from PTE contamination, ii) identify the sources, transport and precipitation processes of PTEs and iii) investigate the traces of natural events (volcanic eruptions, etc.) and paleoecological conditions in the Black Sea sediments during geological periods in a study area of 1200 km in east-west direction along the southern shores of the Black Sea. The study differs from the existing studies as it is the most comprehensive ecological risk research initiative conducted on the Black Sea coasts in line with the aforementioned purposes.

1.1. Material – method

1.1.1. Sampling and analytical methods

Core samples were taken from 6 points at water depths ranging from 80 to 2000 m along the 1200 km line in Turkish territorial waters on the southern shores of the Black Sea. Sampling points were chosen in accordance with the current systems and stream entrances of the Black Sea. West Black Sea 1 (WBS-1) is on the route of the currents coming from the Sea of Marmara. West Black Sea 2 (WBS- 2) and East Black Sea 1 (EBS-1) are located in the current centers descending from the surface to deep. Middle Black Sea 1 (MBS-1), Middle Black Sea 2 (MBS-2) and East Black Sea 2 (EBS-2) are located at the mouths of the rivers draining the Anatolian land (Fig. 1). The surface sediments of the cores were sliced at 1–5 cm intervals according to water content of samples and the rest of the samples were sliced at 10 cm intervals. All samples were taken to the laboratory under appropriate storage conditions at + 4 °C. The cores were evaluated by dividing them into three different sections as lower, middle and upper sections according to major changes in element contamination (Fig. 2).

Chlorophyll degradation products (CDP) analysis was performed by applying acetone extraction in wet sediment samples (Lorenzen, 1971). The sediments dried at 60 °C for 24 h were pulverized and passed through an 11 mesh sieve. Walkley Black Titration method was used for

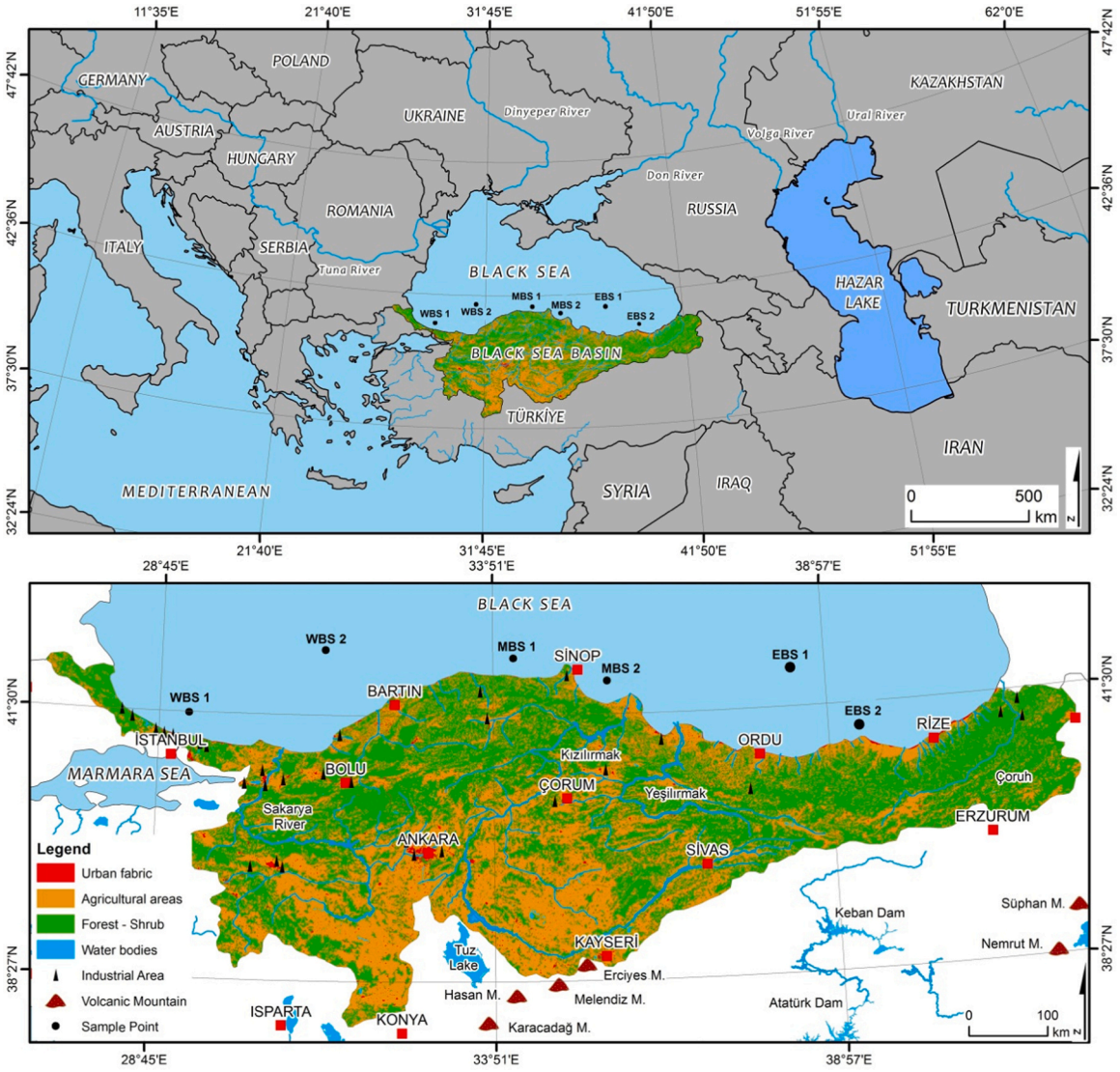

Fig. 1. Location and sampling points of the southern basin of the Black Sea.

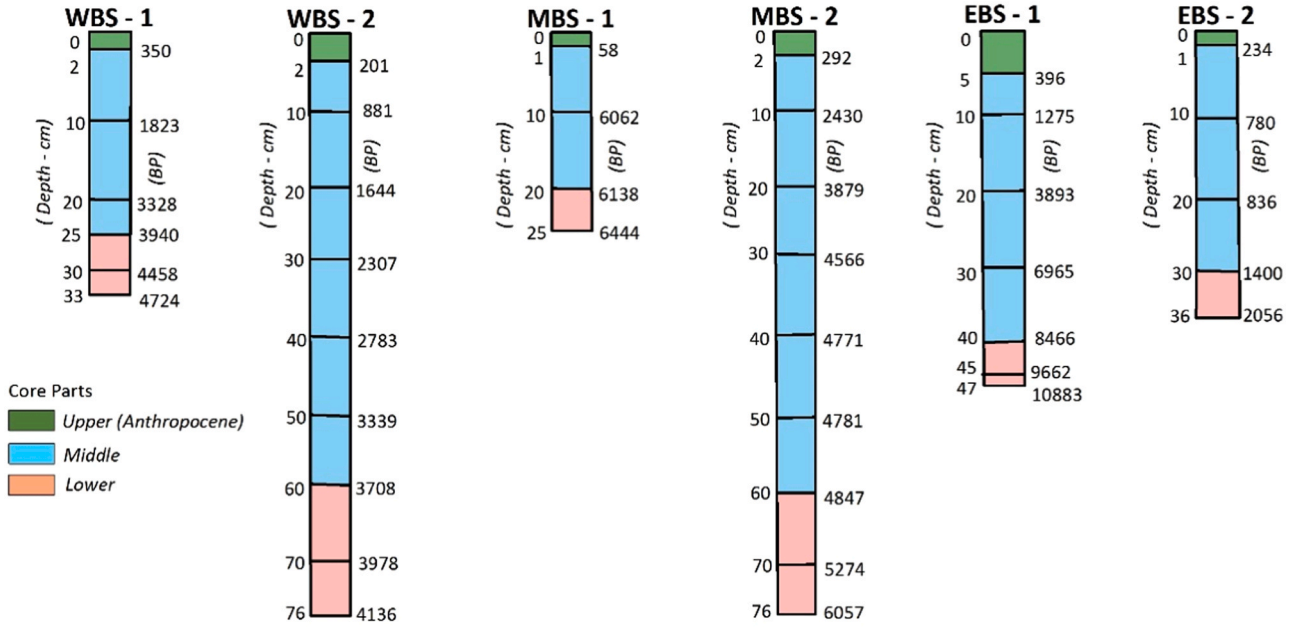

Fig. 2. Ages and sections of cores.

total organic carbon (TOC) analysis (Gaudette et al., 1974). CO_3^{-2} analysis was performed by Scheibler calcimeter (Schlichting and Blume, 1966) and BSi analysis was performed according to De Master (1981). Multi-element analyzes were performed by ICP-MS at the accredited Bureau Veritas Laboratory (Canada). The prepared sample was digested with a modified aqua regia solution with equal parts of concentrated HCl, HNO3, and DI H2O for 1 h in a heating block at 95 °C. The sample was made up to volume with 5% HCl. An internal reference sample (STD OREAS45EA), duplicate measurements, and blank samples were used for quality control of the analyses. Recovery rates varied between 99.26% and 106.67%. Dating of sediment samples was performed with bulk organic material in the Beta Analytic Laboratory (Miami, FL) using the AMS ^{14}C method. Samples for AMS radiocarbon dating were taken from the following depths: 20 and 30 cm for WBS-1, 20, 30 and 76 cm for WBS-2, 10 and 25 cm for MBS-1, 30, 60 cm for MBS-2 and 76 cm, 20, 30 and 47 cm for EBS-1, 10, 20 and 30 cm for EBS-2. "The data obtained from AMS radiocarbon measurements were plotted using calendar calibration, and subsequently, age-depth curves were expressed using polynomials. Using these equations, ages at other levels of the core were predicted through interpolation.

1.1.2. *Multiparametric Approaches*

The enrichment factor (EF) was used for the separation of natural - anthropogenic sources of elements and was calculated according to formula 1 (Sutherland, 2000). Fe, Ti or Al, which are the conservative elements of the earth's crust, are used in order to minimize the error due to grain size in the sediment in the calculation of EF (Zhang et al., 2007). In this study, Al was used as a conservative element for the geochemical normalization process.

It is very important to determine the background values of the elements correctly in enrichment factor calculations. Since each region has its own unique geochemical structure, backgrounds should be determined regionally. There are two ways to do this: either the elemental contents of the bedrock in the region are used, or the values of the pre-pollution period in the core sediments. Using continental crust values in EF calculations may lead to misleading results (Fural et al., 2020). For this reason, different background values were calculated for the elements for which EF values were calculated in all cores. In this way, the background value determined for each station was ensured to represent that region. The minimum element concentrations determined after geochemical normalization was applied to the cores were accepted as the background value. Errors due to grain size were standardized with geochemical normalization.

$$EF = \frac{\left(\frac{C_i}{C_{ref}}\right)_{sample}}{\left(\frac{B_i}{B_{ref}}\right)_{background}} \quad (1)$$

In the EF formula; C_i is element concentration, C_{ref} is the reference element concentration used for normalization, B_i is the regional background value of the element and B_{ref} is the background value of the Al selected for normalization. After applying geochemical normalization with the reference element in the core, the minimum element concentrations were accepted as the background value. A separate background value was calculated for each core.

The modified ecological risk index (mRI) was used to determine the individual ecological risk levels of PTEs (Hakanson, 1980; Brady et al., 2015). mRI was calculated according to formula 2.

$$mRI = EF \text{ x } Tr_i \quad (2)$$

In the formula; EF is the enrichment factor and Tr_i is the toxic risk coefficient of the PTEs. Toxic risk coefficients are as follows: Hg = 40, Cd = 30, As = 10, Cu = Pb = Ni = 5, Cr = 2, Zn = 1, Mn = 1. The modified potential ecological risk index (mPER), which is the sum of the mRI values and which indicates the total ecological risk, was calculated according to formula 3 (Hakanson, 1980; Brady et al., 2015).

$$mPER = \sum_{i=1}^{n} = mER \quad (3)$$

The Toxic Risk Index (TRI) was used to determine the toxic effect levels of the PTEs (Zhang et al., 2016). The individual toxic risk coefficient of PTEs (TRI_i) was determined according to the formula 4.

$$TRI_i = \sqrt{\frac{((C_i/TEL)^2 + (C_i/PEL)^2)}{2}} \quad (4)$$

In the formula; C_i represents the PTE concentration, TEL represents the "threshold effect level" and PEL represents the "probable effect level" (Mac Donald et al., 2000).

Toxic risk index (TRI), showing the total toxic risk, was calculated according to formula 5.

$$TRI = \sum_{i=1}^{n} = TRI_i \quad (5)$$

In the formula; TRI_i represents the individual toxic risk coefficient of the PTEs, $_i$ represents the PTE concentration, ^{n} represents the number of PTEs used in the analysis, and TRI represents the total toxic risk value. The findings obtained from the indices were evaluated according to Table 1.

2. Results and discussion

2.1. Core Ages

The International Commission on Stratigraphy has divided the Holocene epoch into three parts, from lower to upper, as Greenlandian Stage/Age (BP 11.7- 8.2 thousand years), Northgripian Stage/Age (BP 8.2–4.2 thousand years) and Stage/Age Meghalayan (BP 4.2 thousand years- to present / 1950) (Kazancı, 2018). Accordingly, EBS-1 shows the level of PTE contamination and ecological risk from Greenlandian to the present; WBS-1, EBS-1 and EBS-2 shows the level of PTE contamination and ecological risk from the Northgripean to the present and WBS 2 and EBS-2 show the level of PTE contamination and ecological risk from Meghalayan to the present (Fig. 2).

2.2. Temporal variation of PTE, TOC, CDP, BSi and CO_3^{-2} concentrations

WBS-1 core reveals an increasing trend in almost all elements, except As and Cd, from approximately 20 cm towards the surface of the core. As and Cd exhibit minor fluctuations in the lower sections of the core, their most significant increases occur at the surface level. This pattern suggests substantial anthropogenic discharges of these elements into the sea. While not as sharp as As and Cd, an increasing trend is also observed in the surface sediment for Zn, Ni, Fe, and P . However, the rising trends of Cu, Pb, Hg, Al, and Cr elements, which commence at 20 cm depth, exhibit a reversal at the surface (Fig. 3a).

At WBS-2 station, the common increases in elements predominantly occur around 50–60 cm depth. Above 40 cm, except for As, fluctuations are minor. As exhibits an increase at the 20 cm level. Pb, Zn, Ni, Cr, Fe, , Al, and Mn show peaks at 60 cm, whereas Cd, P, and Hg display significant peaks at 50 cm (Fig. 3b).

In station MBS-1, there is no common trend among elements. Cu, Zn, Fe, As, Al, and Cr elements show a decreasing trend in the 0–10 cm range, while Pb, Ni, Cd, Mn, and P show an increasing trend at the surface. Hg, however, exhibits its own fluctuations outside these two groups (Fig. 3c).

At MBS-2 station, Cu, Zn, Cd, and TP exhibit an increasing trend above 40 cm towards the surface, while Mn, Cr, and Ni elements show a decreasing trend. Pb and Hg maintain a relatively stable trend below the surface but exhibit a remarkable peak in surface sediment. The increase in Al at the surface is also noteworthy (Fig. 4a).

EBS-1 core generally displays common trends in the distribution of elements. Common peaks are observed at 20 cm for Cu, Pb, Zn, Ni, and Cd. Fe, Al, and Cr elements exhibit similar distributions throughout the core. While Hg shows a relatively stable trend along the core, it initiates an increasing trend from 15 cm, culminating in a peak at 10 cm, followed by a decreasing trend towards the surface. Mn, on the other hand, demonstrates a regular decreasing trend from the base of the core to 20 cm, followed by an increasing trend towards the surface (Fig. 4b).

In the EBS-2 core, Pb, Zn, and Fe elements show minor fluctuations, indicating an increasing trend from the base to the surface., but this trend reverses at the surface. Other elements exhibit fluctuations along the core and do not show a regular trend. Cu, Ni, As, Cr, and P elements increase their concentrations in surface sediments (Fig. 4c).

The averages of PTEs in six surface sediment cores taken from the southern coast of the Black Sea were compared with those from various coastal regions worldwide. Elevated concentrations of Cu, Ni, Fe, Cd, and As were notable. Cu concentration was found to be higher than that of all other coasts except the Al-Khobar Coast and Montenegrin Coast. Ni and Fe concentrations surpassed those of all other coastal regions. Cd and As concentrations were higher than those in other coastal regions, except for the Montenegrin Coast. A detailed comparison of other PTEs is provided in Table 2.

The CO_3^{-2} concentration was found to be maximum (32.21%) in the middle part of WBS- 2 (BP 201 - 3708) and minimum in the middle part of EBS-2 (BP 234 - 1400) (Figs. 3b and 4c). The CO_3^{-2}concentration that tended to increase towards the surface in WBS-1, WBS- 2 and MBS-2 tended to decrease in the other cores. The probable reason of the increasing trend of CO_3^{-2} concentration on the surface of the WBS-1, WBS-2 and EBS-2 cores may be the discharge of CO_3^{-2} into the Black Sea by the rivers because WBS-1 is under the influence of the rivers in the north of Istanbul, WBS- 2 is under the influence of the Sakarya River, and MBS-2 is under the influence of the Kızılırmak (Fig. 1). These river basins are areas where CO_3^{-2} containing rock formations are common (MTA, 2022).

TOC concentration was found to be maximum (11.77%) in the middle part of EBS - 1 (BP 396 - 9662), and minimum (0.22%) in the middle part of MBS-2 (BP 202 - 4847). TOC tended to increase in the upper sections of all cores except MBS-1 and EBS-2 (Figs. 3c and 4c). This shows that the amount of TOC has started to increase in the Black Sea region in recent years due to industry and urbanization. The decrease in surface sediments in EBS-2 is due to phosphate in the water column limiting algal growth.

CDP concentration was found to show an increasing trend in the upper part of all cores except MBS-2 and EBS-1. The maximum CDP concentration (1121 μg/gr) was found in the middle part of EBS-1 (BP 396 - 9662), while the minimum CDP concentration was found in the upper part of MBS-1 (BP 0 - 58). This increase in CDP concentration in the EBS-1 core is thought to be related to climatic factors. As a matter of fact, TOC values showing similar changes in the same core support this view.

The BSi concentration was found to be maximum (12.84%) in the upper part of EBS-1 (BP 0 - 396) and minimum (2.16%) in the upper part of WBS-1 (BP 0 - 350). BSi, with a tendency to increase on the surface of MBS-1 and EBS-2, tended to decrease in other cores. Figs. 3 and 4 presents the temporal variations of all variables in detail. The contrast between the BSi increase in the EBS-1 core surface and the CDP and TOC values at the same level may indicate that these variables have different sources. CDP and TOC are thought to be of terrestrial origin, while BSi is of marine origin.

Table 1
Index Scales.

Enrichment Factor		Modified Ecological Risk Index	
EF	**(Sutherland, 2000)**	**mRI**	**(Hakanson, 1980).**
< 2	Deficiency to minimal enrichment	**< 40**	Low ecological risk
2 – 5	Moderate enrichment	**40 ≤ mRI < 80**	Moderate ecological risk
5 - 20	Significant enrichment	**80 ≤ mRI < 160**	Significant ecological risk
20 – 40	Very high enrichment	**160 ≤ mRI < 320**	High ecological risk
> 40	Extremely high enrichment	**≥ 320**	Very high ecological risk
Toxic Risk Index		**Modified Potential Ecological Risk Index**	
TRI	**(Zhang et al., 2016).**	**mPER**	**(Hakanson, 1980)**
TRI ≤ 5	No toxic risk	**< 150**	Low potential ecological risk
5 < TRI ≤ 10	Low toxic risk	**150 ≤ mPER < 300**	Moderate potential ecological risk
10 < TRI ≤ 15	Moderate toxic risk	**300 ≤ mPER < 600**	Significant potential ecological risk
15 < TRI ≤ 20	Considerable toxic risk	**mPER ≥ 600**	Very high potential ecological risk
TRI > 20	Very high toxic risk		

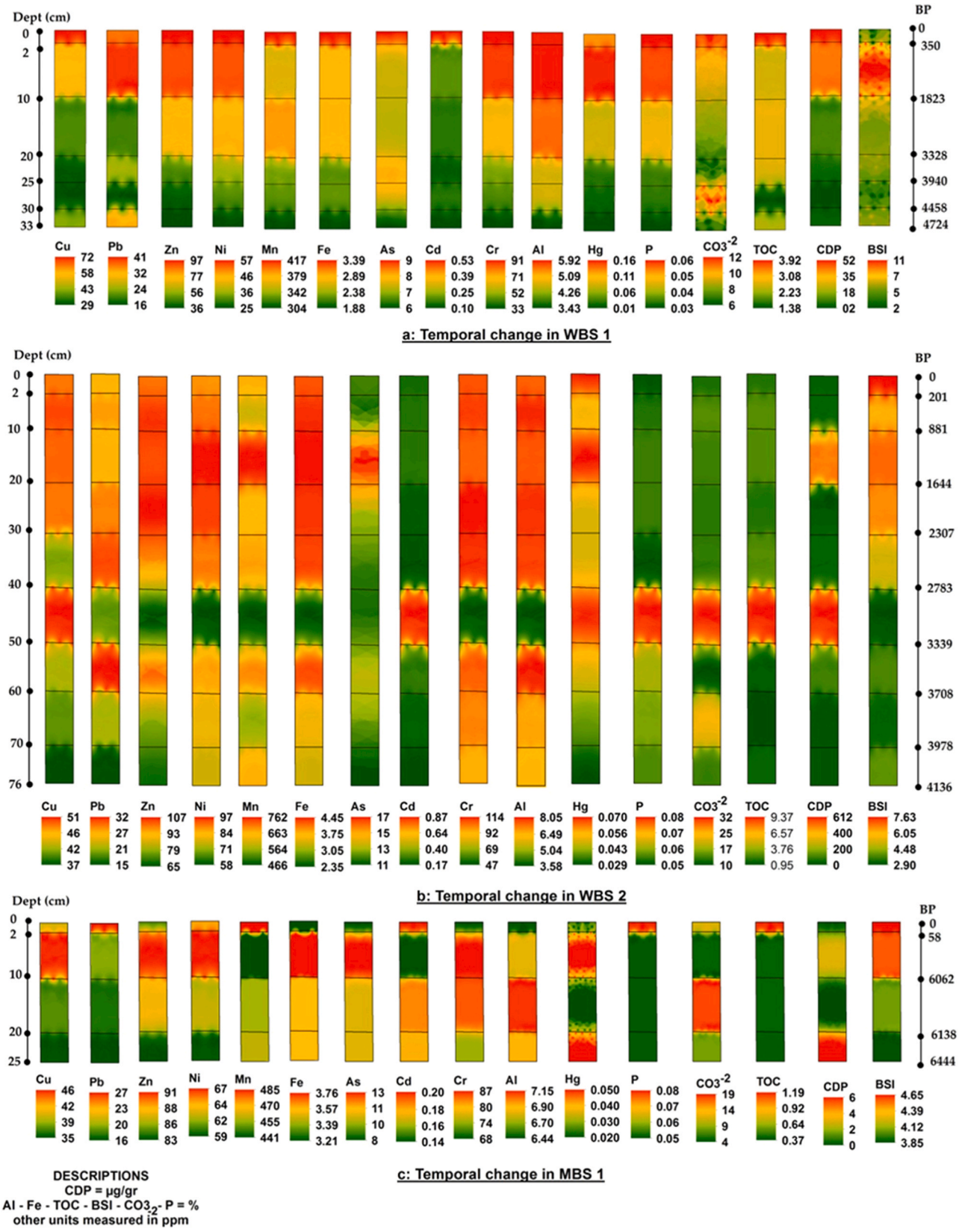

Fig. 3. Temporal variation of PTE, TOC, CDP, BSi and CO_3^{-2} concentrations.

Fig. 4. Temporal variation of PTE, TOC, CDP, BSi and CO3–2 concentrations.

Table 2
Comparison of element concentrations with some coastal areas.

(ppm)	*Cu*	*Pb*	*Zn*	*Ni*	*Mn*	*Fe*	*As*	*Cd*	*Cr*	*Hg*
S. Black Sea Coast[a]	59.62	30.98	99.20	90.33	594	41,500	11.43	0.33	102.67	0.07
Ismailia Canal[b]	32.64	31.78	117.00	32.14	194	5200		0.23		
Al-Khobar Coast[c]	180.90	5.33	52.51	75.17	113	7473		0.22		0.80
Red Sea Coast[d]	0.47	2.57	6.74	2.44	909	4168		0.09		
Montenegrin Coast[e]	154.00	70.30	234.00	83.30	634	23,400	12.30	0.65	97.60	0.77
Caspian Sea[f]	21.87	15.98	73.22	47.71			10.37		127.38	
Yellow Sea[g]	20.03	23.33	65.97	26.69			9.92	0.20	59.06	0.02
Adriatic Sea[h]	11.58	218.00	410.00	27.77	676			0.22	28.65	0.03

[a] This study (Türkiye)
[b] Nour et al. (2022) (Egypt)
[c] Al-Kahtany et al. (2023a) (Saudi Arabia)
[d] Al-Kahtany et al. (2023b) (Egypt)
[e] Joksimović et al. (2020) (Montenegro)
[f] Bastami et al. (2015) (Iran)
[g] Xu et al. (2016), (China)
[h] Frontalini and Coccioni (2007) (Italy).

2.3. Temporal variation of EF, mRI, mPER, and TRI

Cu, Zn and Cd were moderately enriched, while Hg was significantly enriched in the upper part of WBS-1 (BP 0 - 350). Pb was moderately enriched in the middle-upper part of WBS-1 (BP 350 - 3940) in Meghalayan (BP 0 - 4.2 thousand years). Hg was moderately enriched in lower part of WBS-1 (BP 3940 - 4724), representing the beginning of the Northgripian period (BP 8.2–4.2 thousand years). No enrichment was detected in any part of WBS-1 for Ni, Cr, Mn, As and Al, indicating that these elements come from natural sources. The EF values of the PTEs other than As and Cd, which were enriched at various levels in different parts of WBS-1, have a tendency to decrease today. However, Cd enrichment tended to increase sharply in the last 200 – 300 years (Fig. 5a). The enrichments observed in the post industrial period can be explained by human influence, while the enrichments observed during the Northgripian and Meghalayan periods can be explained by paleo-ecological conditions.

According to mRI data; Cd caused a moderate ecological risk in the lower (BP 3940 - 4724) and middle (BP 350 - 3940) parts of WBS-1 and a significant ecological risk in the upper part of WBS-1. On the other hand, Hg created a moderate ecological risk in the lower part (BP 3940 - 4724), a significant ecological risk in the middle part (BP 350 - 3940) and a high degree ecological risk in the upper part of WBS-1 (BP 0 - 350). No ecological risk hazard has been identified for the other PTEs. The increasing ecological risk level of Hg and Cd draws attention. mPER data showed a medium-significant potential ecological risk in the middle part (BP 350 - 3940) and significant potential ecological risk in the upper part of WBS-1 (BP 0 - 350). Potential ecological risk generally increased from the lower part of the core to the middle part but has a tendency to decrease today. According to TRI data, no toxic risk was found in the lower part of WBS-1 (BP 3940 - 4724), but a low toxic risk was detected in the middle (BP 350 - 3940) and upper part (BP 0 - 350). The toxic risk tends to increase continuously from the lower part of the core to the present (Fig. 7a).

Significant Cd enrichment and moderate Hg enrichment were detected in the middle section of WBS 2 (BP 201 - 3708), which represents the Meghalayan period. Today, Cd enrichment tends to decrease, while Hg enrichment tends to increase (Fig. 5b). According to mRI values, Cd was high in the middle section of WBS 2 (BP 201 - 3708), while Hg created a significant ecological risk. Hg posed moderate ecological risk in the upper (BP 0 - 201) and lower sections of WBS 2 (BP 3708 - 4136). Although the ecological risk level of Hg decreased to the moderate level in the upper part of the core, the ecological risk level tends to increase nowadays. Toxic risk index values (TRI) indicate low toxic risk in all sections of WBS 2. mPER shows an increasing trend towards the surface in the WBS 2 core, while TRI shows an almost stable appearance. The likely source of increased element enrichment and potential ecological risk during the mid-Meghalayan period was paleo-ecological conditions (Fig. 7b) since there were any anthropogenic activities in the region during the Meghalayan period.

The lower section (BP 6138 - 6444) of MBS-1 represents the Northgripian, while the middle (BP 58 - 6138) and the upper section (BP 0 - 58) represent the Meghalayan period. No enrichment was detected for any PTEs in MBS-1. However, the enrichment level of Pb, Zn, Ni, Cd, Cu started to increase in the post-industrial period (Fig. 5c). This indicates the existence of anthropogenic sourced discharges near MBS-1. A moderate ecological risk from Cd and Hg was detected in the upper section of MBS-1 (BP 0 - 58). It is noteworthy that Hg caused moderate ecological risk throughout the core. The ecological risk level of Cd tended to increase in the last 200 – 300 years. Potential ecological risk indexes also tended to increase in the upper section of the core (BP 0 - 58), indicating the increase of anthropogenic effects in MBS-1 (Fig. 7c).

The lower section of the MBS-2 core (BP 4847 - 6057) taken at the mouth of the Kızılırmak River, which drains an important urbanization, agriculture and industry basin in Türkiye, represents the Northgripian period, while the middle (BP 202 - 4847) and the upper sections (BP 0 - 202) represent the Meghalayan period. Moderate Hg enrichment was detected in the upper section of MBS-2. Pb approached the moderate enrichment limit in the post-industrial period (Fig. 6a). In addition to Hg and Pb, Cu enrichment showed an increasing trend in that period. The studies conducted in the Kızılırmak basin pointed to significant anthropogenic PTE contamination (Bilhan and İlalan, 2021). This is an important proof that the anthropogenic effects in the basin directly affect the Black Sea. Cd was found to pose a moderate ecological risk in the middle (BP 202 - 4847) and upper sections (BP 0 - 202) of MBS-2. Hg created a moderate ecological risk in the lower (BP 4847 - 6057) and middle sections of MBS-2, and a significant ecological risk in the upper section. The ecological risk level of Cu, Pb and Hg rapidly increased in the upper parts of cores. Therefore, contaminations of Cu, Pb and Hg around MBS-2 should be carefully monitored. A moderate toxic risk was identified in all sections of MBS-2. Moderate potential ecological risk was detected in the upper section of MBS-2. It is noteworthy that the toxic risk and potential ecological risk in MBS-2 tended to increase in the in the last two or three centuries, which represents the upper section of the core (BP 0 - 202) (Fig. 8a). This indicates that the discharge of PTE from terrestrial sources of anthropogenic origin continues.

The oldest core of the study area was identified as EBS-1. The lower section of the core (BP 9662 - 10883) corresponds to the late Greenlandian period and the middle section (BP 396 - 9662) corresponds to the Northgripian period. Cd and Hg were moderately enriched in the upper section of EBS-1 (BP 0 - 396). Cu, As, Hg, and Cd were moderately enriched in the middle section that represented the Northgripian period.

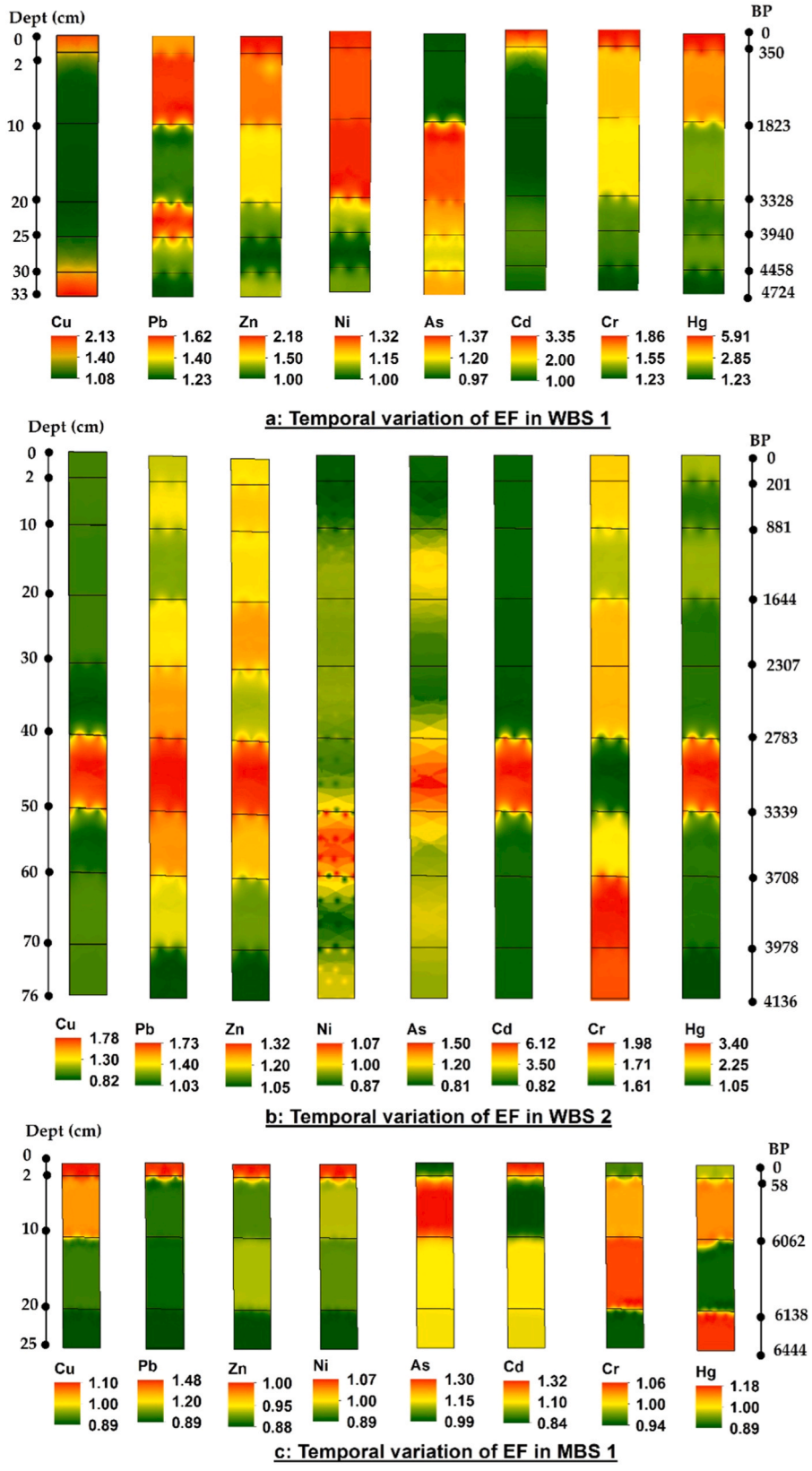

Fig. 5. Temporal variation of EF.

Cr were moderately enriched in the lower section that represented the Greenlandian period (Fig. 6b). A moderate to significant Cd and Hg ecological risk was detected in the middle section of EBS-1 (BP 396 - 9662). The ecological risk of Cd and Hg tends to decrease nowadays. Although a moderate to significant potential ecological risk was detected in the upper (BP 0 - 396) and middle sections of EBS-1, it is noteworthy that the downward trend began in the surface. The reason for this decrease may be related to the decrease of Cd and Hg enrichment

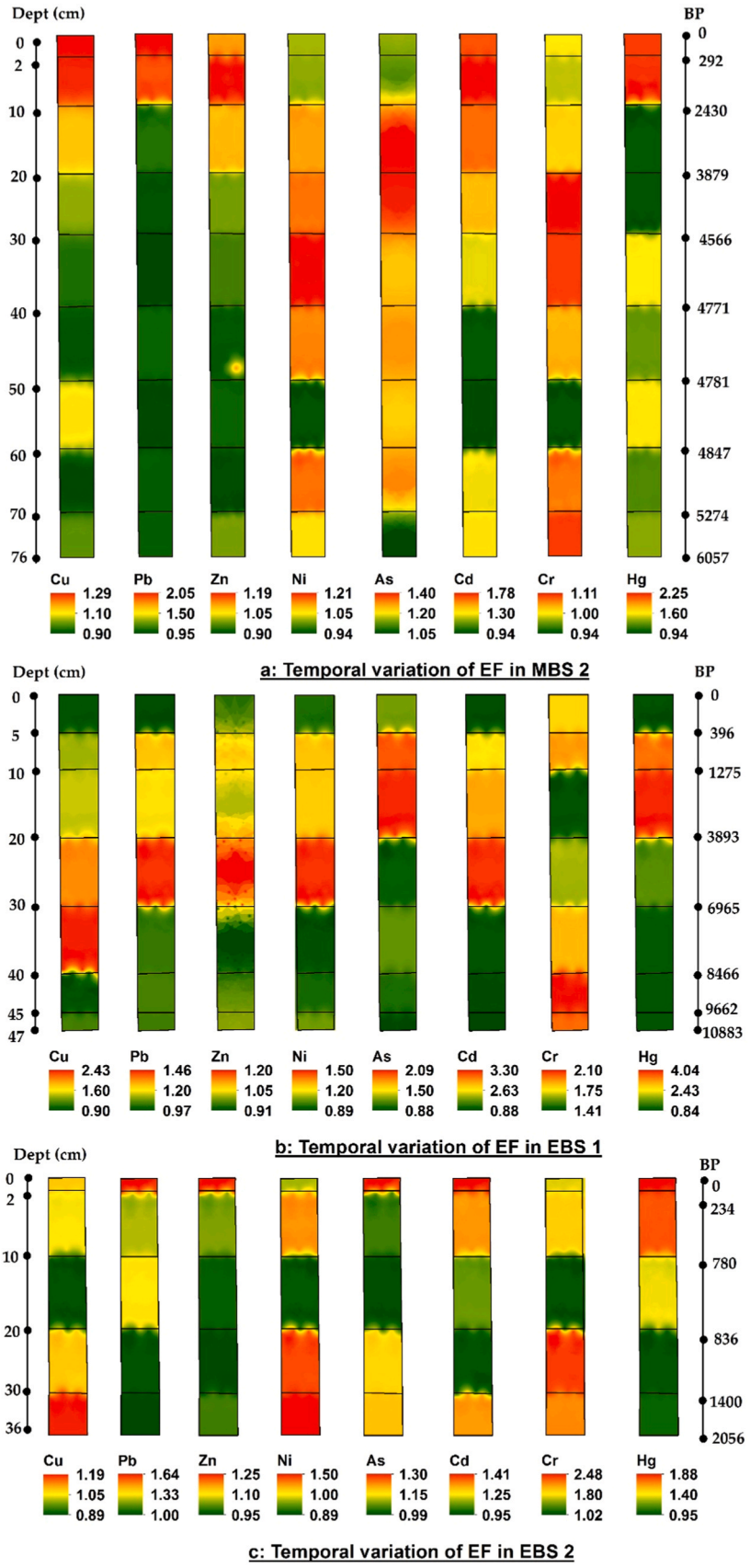

Fig. 6. Temporal variation of EF.

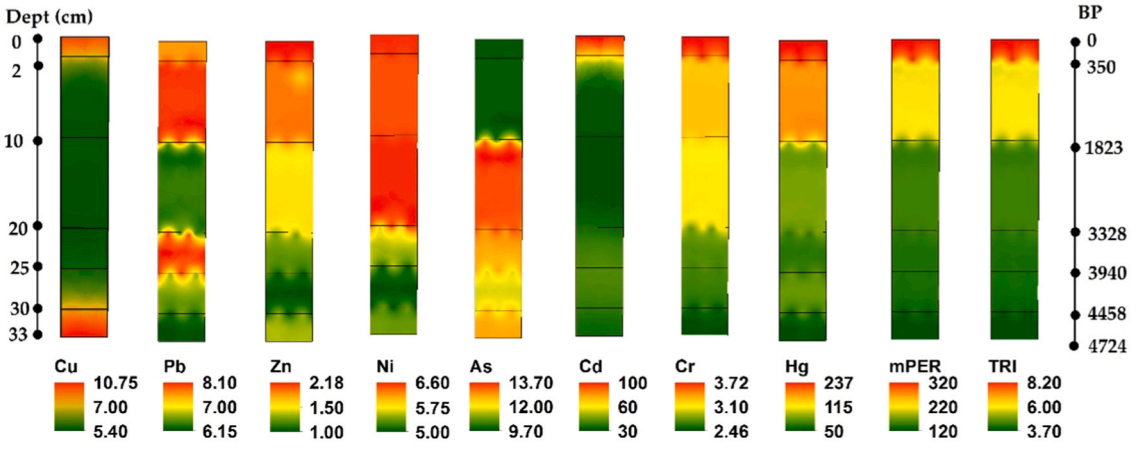

a: Temporal variation of mRI, mPER, and TRI in WBS 1

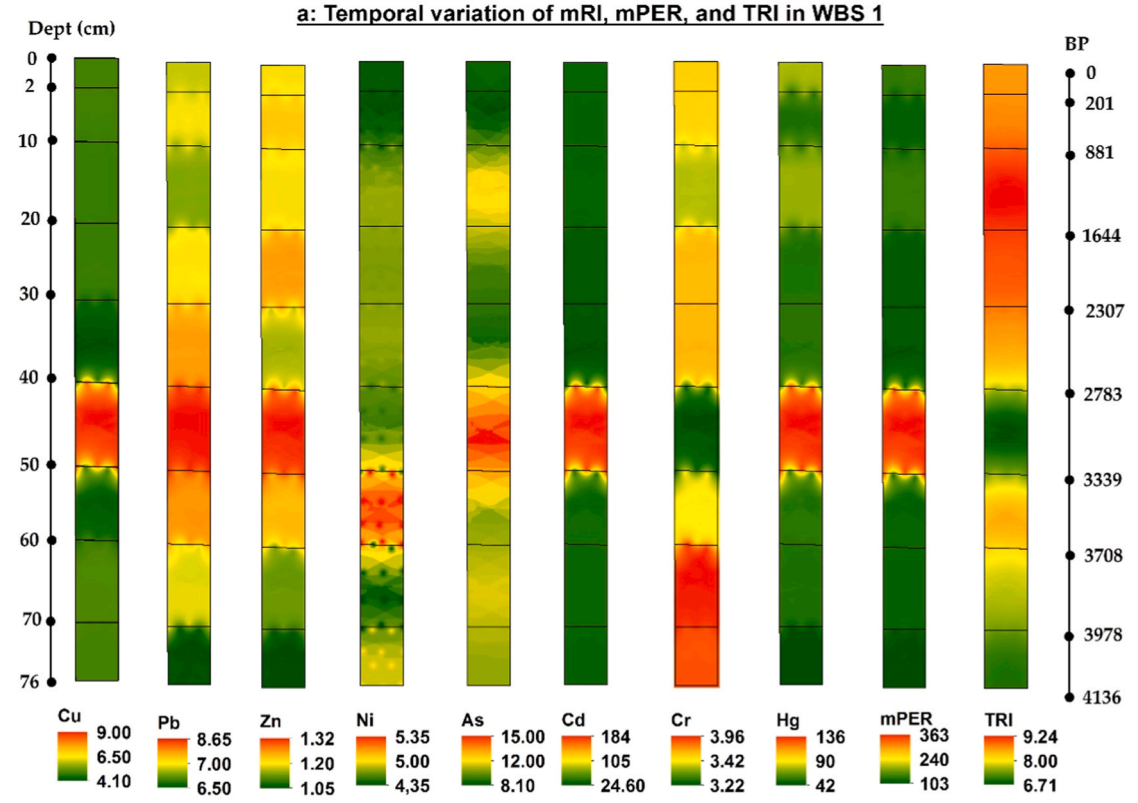

b: Temporal variation of mRI, mPER, and TRI in WBS 2

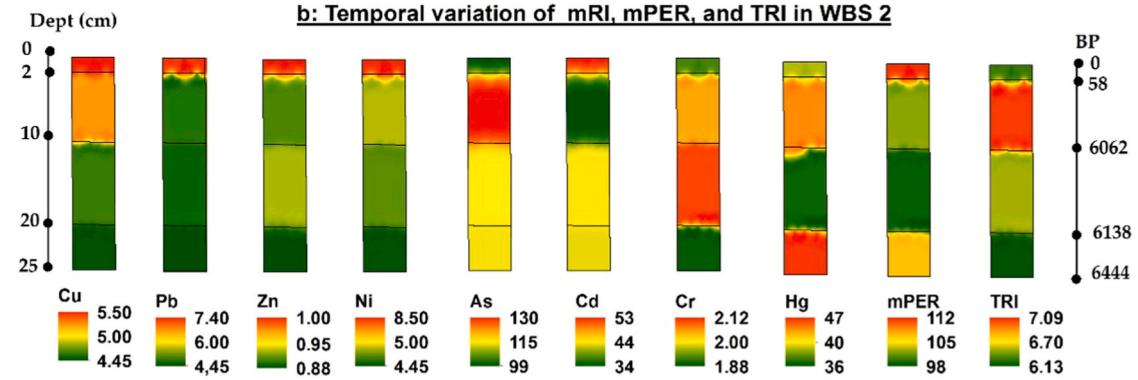

c: Temporal variation of mRI, mPER, and TRI in MBS 1

Fig. 7. Temporal variation of mRI, mPER, TRI.

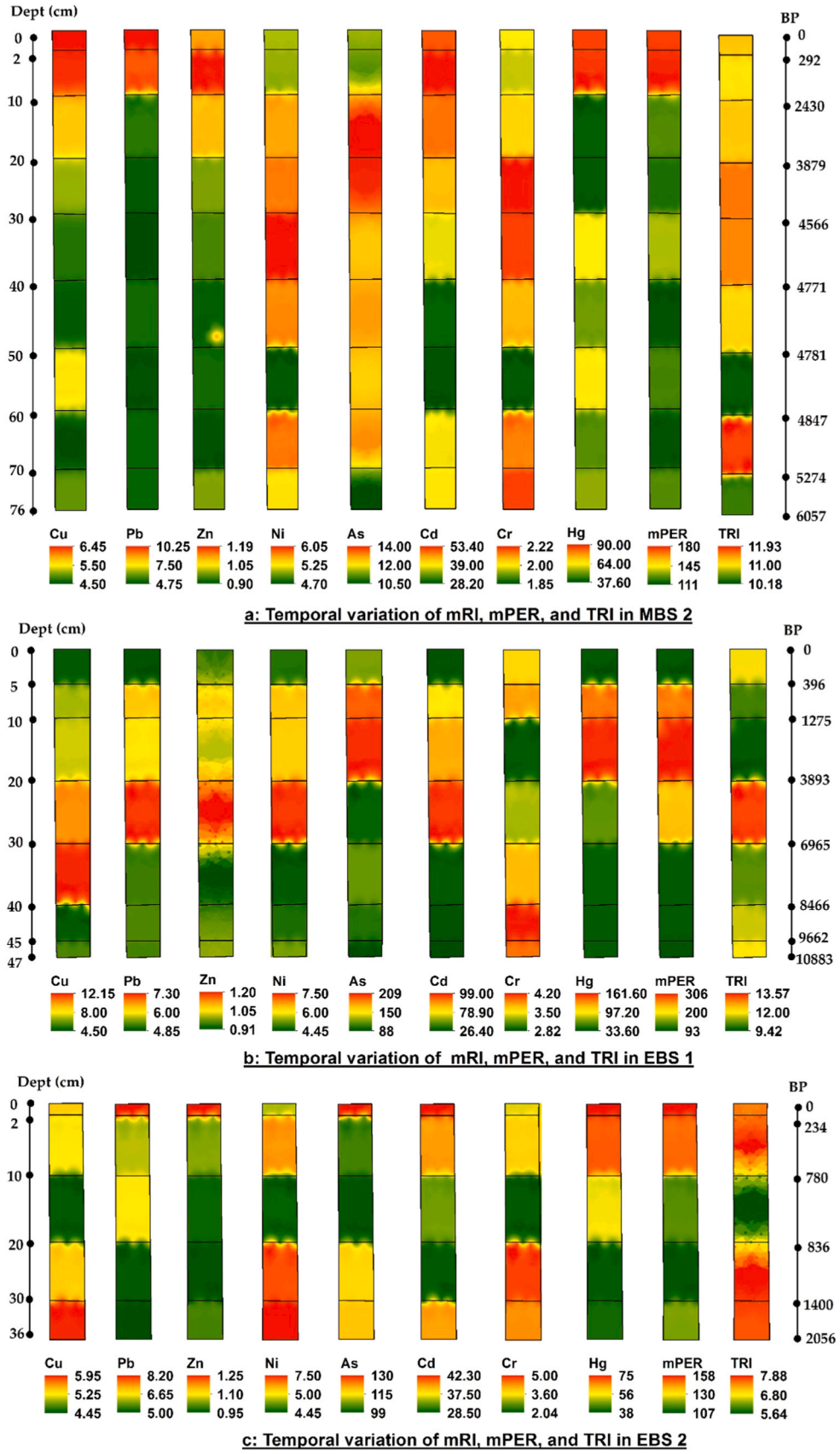

Fig. 8. Temporal variation of mRI, mPER, TRI.

towards the surface. Toxic risk was found to be moderate in all sections of the core. The level of toxic risk remained almost constant in the recent years (Fig. 8b).

All EBS-2 sections represent the Meghalayan period. Moderate Ni and Cr enrichment was detected in the middle (BP 234 - 1400) and lower sections (BP 1400 - 2056) of the core (Fig. 6c). Moderate Hg ecological risk was detected in all parts of EBS-2. Cd created a moderate ecological risk in the middle and upper sections of the core (BP 0 - 234). The ecological risk level of Cu, Ni, As, Cr and Hg tended to increase in the last few years. Toxic risk was low in all sections of the core. However, it is noteworthy that the toxic risk level tended to increase in recent years. The potential ecological risk was found to be moderate in the middle and upper sections of EBS-2 and it continues to increase today (Fig. 8c).

Based on the assessment of all cores, it is observed that As, Cu, Pb, Zn, Cd, Hg, Ni enrichment increased in the recent past in the Black Sea. Anthropogenic effects were detected most in the core coded WBS-1 which was taken from the northern coast of Istanbul and the the core coded MBS-2 which was taken from the mouth of the Kızılırmak mouth. The source of moderate Cu, Zn and Cd and significant Hg enrichments in WBS-1 during the last 350 years.

Hg enrichment in MBS-2 and the related ecological risk level were observed to be noteworthy. mRI findings pointed to Hg and Cd as the main PTEs posing a moderate to significant ecological risk across the Black Sea. According to the research findings, the integrated potential ecological risk is concentrated in over the last few years. This provides evidence that human activities in the Black Sea basin have an impact on ecosystem degradation.

2.4. Source apportionment

One of the two most risky cores in terms of ecological risk and PTE contamination was identified to be WBS-1. WBS-1 is located in the Black

Table 3
Results of factor analysis.

Table 3a: Factor Analysis of WBS 1

	Fac. 1	*Fac. 2*	*Fac. 3*
TOC	0.306	-0.025	0.914
CDP	0.829	-0.027	0.385
BSi	0.138	-0.732	0.432
Cu	0.892	-0.083	0.192
Pb	0.981	0.026	-0.079
Zn	0.949	0.001	0.228
Ni	0.927	0.030	0.349
Mn	0.676	0.361	0.483
Fe	0.851	0.258	0.351
As	-0.178	0.813	0.291
Cd	0.615	0.551	0.315
P	0.931	0.094	0.309
Cr	0.972	0.010	0.194
AI	0.896	0.168	0.111
Hg	0.971	-0.097	0.008
CO3-2	0.200	0.718	-0.044

Table 3b: Factor Analysis of WBS 2

	Fac. 1	*Fac. 2*	*Fac. 3*	*Fac. 4*
CO3 − 2	-0.936	-0.133	-0.053	-0.116
TOC	-0.855	0.249	0.018	0.402
CDP	0.048	-0.194	0.017	0.928
BSi	0.669	0.682	-0.079	-0.122
Cu	-0.058	0.898	-0.120	-0.005
Pb	0.803	-0.152	0.083	0.275
Zn	0.926	0.141	0.121	0.103
Ni	0.905	0.035	0.250	0.107
Mn	0.767	0.082	0.527	-0.119
Fe	0.979	0.066	0.139	0.012
As	0.123	0.010	0.942	0.042
Cd	-0.909	0.336	-0.057	0.066
P	-0.899	-0.166	0.072	0.112
AI	0.973	-0.150	0.068	0.007
Hg	-0.181	0.819	0.261	-0.215

Table 3c. Factor Analysis of MBS 1

	Fac. 1	***Fac. 2***	***Fac. 3***	***Fac. 4***
CO3 − 2	-0.080	-0.025	-0.302	0.876
TOC	-0. 783	0.182	-0. 059	0.054
CDP	-0.302	0.835	0.040	-0.364
BSi	0.219	0.758	0.257	0.254
Cu	0.102	-0.087	0.892	-o. 183
Pb	-0.674	-0.390	0.525	0.210
Zn	0.694	0.318	0.559	0.127
Ni	0.122	0.180	0.743	-0.236
Mn	-0.825	-0.268	-0.178	0.224
Fe	0.937	0.141	0.004	-0.271
As	0.874	0.242	0.185	-0.220
Cd	-0.615	0.201	-0.085	0.685
P	-0.856	0.060	0.019	0.088
Cr	0.915	0.191	0.175	0.066
AI	0.522	0.747	-0.269	0.036
Hg	0.580	0.445	0.106	-0.589

Table 3d: Factor Analysis of MBS 2

	Fac. 1	***Fac. 2***	***Fac. 3***	***Fac. 4***
CO3 − 2	0.150	-0.078	-0.003	0.943
TOC	0.015	-0.829	-0.193	0.286
CDP	0.680	-0.172	0.199	-0.436
BSi	0.842	-0.226	0.355	-0.012
Cu	0.874	-0. 292	-0.072	0.021
Pb	0.890	-0.195	0.345	-0.029
Zn	0.957	-0.196	-0.172	0.030
Ni	-0.304	0.882	-0.045	0.135
Mn	-0.855	0.234	-0.077	-0.059
Fe	-0.202	0.770	0.477	-0.034
As	-0.172	0.788	-0.189	-0.090
Cd	0.844	-0.171	-0.369	0.289
P	0.937	-0.187	-0.107	0.093
Cr	-0.425	0.706	0.004	0.322
Al	-0.445	0.334	0.754	-0.117
Hg	0.454	-0. 110	0.819	0.038

Table 3e: Factor Analysis of EBS 1

	Fac. 1	***Fac. 2***	***Fac. 3***
CO3 − 2	-0.751	-0.292	0.070
TOC	-0.437	0.719	-0.086
CDP	-0.059	0.925	0.165
BSi	0.227	0.001	0.882
Cu	0.127	0.922	0.028
Pb	0.698	0.635	-0.057
Zn	0.920	-0.029	0.245
Ni	0.564	0.514	0.238
Mn	0.701	-0.360	-0.493
Fe	0.830	-0.386	0.149
As	-0.286	-0.779	0.388
Cd	-0.398	0.727	0.350
P	0.752	0.294	0.124
Cr	0.913	-0.352	-0.130
AI	0.900	-0.111	-0. 106
Hg	-0.942	-0.057	-0. 125

Table 3f: Factor Analysis of EBS 2

	Fac. 1	***Fac. 2***	***Fac. 3***	***Fac. 4***
CO3 − 2	-0.159	0.018	0.743	0.176
TOC	-0.617	0.360	-0.444	-0.008
CDP	-0.151	0.786	-0.239	0.053
BSi	0.775	0.072	0.212	-0.040
Cu	0.178	0.745	0.420	0.331
Pb	0.833	-0.429	-0.233	-0.070
Zn	0.826	-0.340	-0.129	0.109
Ni	-0.322	0.717	0.397	0.271
Mn	-0. 339	0.406	0.268	0.731
Fe	0.806	-0.166	0.035	0.056
As	0.104	0.652	0.506	-0. 300
Cd	0.732	0.070	-0.283	0.058
P	0.729	0.340	0.446	0.136
Cr	0.027	0.168	0.784	0.010
AI	0.484	-0.006	0.019	0.828
Hg	0.920	0.067	-0.095	-0.019

Sea in the most open location to anthropogenic effects. The location of the core is influenced by the rivers that discharge to the northern shores of the Black Sea, especially the Danube, because a clockwise current system is dominant in the Black Sea from the littoral zone to the deep parts (Bakan and Büyükgüngör, 2000).

The aforementioned current system carries the waters discharged from the south and north of the Black Sea along the coast. The sampling area where the WBS-1 core was taken is under the influence of the Sea of Marmara as well as the inland current system of the Black Sea. The Sea of Marmara is an extremely problematic inland sea ecologically that carries the anthropogenic burden of approximately 20 million people and important metropolises (Öztürk and Şeker, 2021). The bottom currents advancing from the floor of the Sea of Marmara towards the Black Sea pass through the area where the WBS-1 core is located (Güler et al., 2004). The rivers of the northern basin of Istanbul, which drain into an area close to WBS-1, are under the pressure of other industrial activities, especially mining (Avcı, 2019).

Factor analysis was performed for each core to identify the source of the PTEs. The lithophile elements Al, Fe, Mn were together with moderately enriched Cu, Pb, Zn and moderately to significantly enriched Cd – Hg in Factor 1 which was identified in the factor analysis conducted for WBS-1 (Table 3a). The main source of Hg, Pb, Cu, Zn and Cd were estimated to be domestic and industrial wastes drifted by the undercurrents of the Sea of Marmara. Cu and Zn enrichment in WBS-1 appeared in in the past few years. Pb enrichment appeared before the Meghalian but it does not exist today. Cd enrichment emerged in recent years and continues today. Hg enrichment emerged in the mid-Meghalayan and continues today. In conclusion, Hg and Cd enrichment is the current problem in WBS-1. The probable reason for the Hg and Cd enrichment is the rapidly increasing domestic and industrial waste load around Istanbul.

The decrease in lithophile element concentrations in the periods when Pb, Zn, Cu concentrations increased in WBS-1 strengthens the possibility that the mentioned elements are of terrestrial anthropogenic origin. As and Cd are included in the same factor as well. It is estimated that As and Cd, which are affected by anthropogenic activities, originate from domestic and industrial waste discharge. Diatoms in the aquatic environment decrease with Cd and As contamination. This disrupts the phytoplankton community and decreases the BSi concentration. The CDP concentration increased with the input of P into the aquatic environment. Mn and TOC move together in the suboxic zone. Being carbonate lithophile and anthropogenic may be of dual origin due to the existence of natural clay deposits and mines in the region (MTA, 2022).

WBS 2 was taken from the point located 124 km off the coast, at the east of the Sakarya River mouth, at a depth of 2000 m. Significant Cd and Hg enrichment was detected in the lower section of WBS 2 (BP 3708 - 4136), representing the early Meghalayan period. This enrichment cannot be explained by anthropogenic activity. The source of the element enrichment experienced in the early Meghalayan period may be related to the paleo-environmental conditions of the period.

Factor 1 in WBS 2 consists of positively loaded Pb, Zn, Ni, Mn, Fe, Cr, Al elements. Factor 1 is a complex set of lithophiles and elements of mostly anthropogenic origin. Factor 2 consists of Cd and Hg, affected by natural sources in the early Meghalayan period and anthropogenic sources in the upper section of the core. Factor 2 is a factor of complex origin, but consists of elements that are discharged in different ways (possibly volcanic eruption) compared to other sets/clusters. Factor 3 consists of As, Mn and P (Table 3b). As, generally under the effect of anthropogenic sources, was not enriched in WBS 2. In this case, Factor 3 consists of lithophyll-based elements discharged by rivers via terrestrial erosion. CDP in Factor 4 may have experienced a positive linked concentration increase in the marine environment. WBS 2 is largely under the influence of discharges from the Sakarya River Basin. There are traces of Holocene volcanism on the Ankara Melange and Karacakaya Formation which includes the Sakarya River. In addition, the erosion and transport capacity of Anatolian rivers increased during the Holocene, the interglacial period (Russel, 1954). The enrichment that emerged in a period when human influence was extremely slim is very likely to be related to terrestrial erosion and transport processes. Galatia volcanic region, which was active in the Holocene, is located within the borders of the Sakarya River basin, the Western Anatolia volcanic area. (Atıcı and Türkecan, 2017). In this case, the source of element enrichment in the lower section of WBS 2 is the volcanic activity experienced in the region in the past.

MBS 1 was retrieved from the western part of Sinop, 13.8 km offshore, at a depth of 91 m. No element enrichment was observed in this core; however, there was an increasing trend in Cu, Pb, Zn, and Cd enrichment during the Anthropocene. The potential source of the Cu enrichment trend is the Cu mines in Küre Mountain (Mineral Research and Exploration Department MTA, 2021). Zn and Cd are essential plant nutrients used in agriculture, and Cd can also originate from domestic and industrial waste (Cheng et al., 2013). No lithophilic source for Pb has been identified in the MBS 1 area; thus, the source of Pb is believed to be anthropogenic. A potential source of the Pb enrichment trend is ongoing mining and other industrial activities around the coastal zone (Homens et al., 2013). No anthropogenic impact has been detected in MBS 1 at a level that would create enrichment or ecological risk. The sources of PTEs are complex, and factor analysis supports the current findings.

MBS-2 was taken from a point close to the mouth of the Kızılırmak River, 15 km from the shore, at a depth of 75 m. Pb and Hg were found to be moderately enriched in the upper section of the core corresponding to the Anthropocene. Cd, on the other hand, approached the moderate enrichment limit. The anthropogenic source of the aforementioned elements is domestic and industrial wastes (Homens et al., 2013). Kızılırmak is the largest river and the largest catchment area in Türkiye. Domestic and industrial wastes of many cities are discharged to the Black Sea via Kızılırmak. In factor analysis, Pb and Cd were found to be in the same factor, while Hg was included in a separate factor. The possible source of this difference is the discharge of the elements into the Black Sea via different transport processes.

Factor 1 in MBS-2 consists of Pb and Cd of anthropogenic origin and non-enriched elements. Factor 2 consists of lithophile elements. Factor 3 consists of Hg from anthropogenic origin and Al from lithophile origin. Factor 4 consists of CO_3^{-2} discharged by terrestrial erosion (Table 3d). Elements of anthropogenic origin discharged into streams and elements transported by terrestrial erosion may be included in the same factor. MBS-2 is a very complex core in terms of source and transport processes for two reasons: (1) MBS-2 is under the influence of Kızılırmak, the largest river draining the southern shores of the Black Sea. It discharges the elements affected by different sources in the Kızılırmak basin to the Black Sea. (2) MBS-2 reflects the effects of natural and anthropogenic processes from the mid-Northgripean period (BP 6057) to the present.

EBS-1 was taken at a point located 132 km off the coast, from a depth of 2000 m. Cu, Mn, As, Cd, Cr, Hg were found to be moderately enriched in the middle section of the core (BP 396 - 6935). However, the aforementioned elements were not enriched in recent years. Factor 1 in EBS-1 consists of lithophile elements in line with the Anthropocene conditions. The negative correlation of Hg with all elements in Factor 1 indicates that it was transported from a different source by a different route. It is estimated that Factor 2 originated from agriculture or was formed by the primary producer effect. Factor 3 is estimated to be formed as a result of As transport of diatoms (Table 3e). The probable source of the element enrichment in the middle part of the core, which started from the middle of the Northgripian period and continued in the Meghalayan period, was the volcanic activities that took place especially in Eastern Anatolia and the Caucasus (Atıcı and Türkecan, 2017; Lebedev et al., 2010).

EBS-2 was taken at a point located 4.1 km off the coast, from a depth of 200 m. In EBS-2, elements of lithogenic and anthropogenic origin are combined in Factor 1. Elements may have been transported via diatom in this factor. Pb and Hg were enriched in recent years to a near-moderate level. These two elements are mostly of domestic and

industrial origin (Homens et al., 2013). Factor 2 consists of Cu and Ni. The elements Cu and Ni may be transported by primary producers other than diatoms, such as macroalgae and other phytoplankton groups. Factor 3 is composed of CO_3^{-2} and Cr and is most likely of lithophile origin. Factor 4 consists of Mn and Al and is of lithophile origin (Table 3f). The presence of similar elements in different factors may be related to the transport processes. As, Cu, and Hg enrichment increased in recent years. Cu is an element mined in the Trabzon borders located in the EBS-2 basin (Yılmaz et al., 2007). Possible sources of As and Hg in the Anthropocene are domestic and industrial wastes and other anthropogenic activities.

2.5. Overall evaluation

The sedimentary processes at the WBS-1 station are influenced by the bottom currents of the Danube River and the Marmara Sea. Industrialization and urbanization in Istanbul, as well as mining operations in the Thrace region, constitute fundamental sources of pollution. The WBS-2 core, sampled 124 km away from the coast, is remote from human impact and subject to natural processes. Element increases observed in the middle of the core are consistent with volcanic activities in the Sakarya Basin. Although there is no enrichment posing a risk in the MBS-1 core, there is a tendency for an upward trend in elements, necessitating monitoring of human activities in the region, particularly mining activities in the Küre Mountains. Sedimentation is prevented at this station due to strong bottom transport vectors. The MBS-2 core, taken off the Kızılırmak River, which drains the Kızılırmak Basin containing 18 cities, reflects anthropogenic impacts. The EBS-1 station is located 132 km offshore and is unaffected by human activities. Enrichments observed in the middle portions of the core may indicate traces of volcanic eruptions in Eastern Anatolia and the Caucasus. Enrichments in the upper parts of the Karoun may represent agricultural activities. In the EBS-2 core, diatoms, macroalgae, and other phytoplankton groups play a dominant role in the transport of metals to the bottom. The element distribution in this core reflects a combination of anthropogenic impact and natural weathering. Although anthropogenic impact is not yet at a risk level, there is an increasing trend.

3. Conclusion

The Black Sea experienced significant anthropogenic pressure, especially in the post-industrial period. PTEs, which contain large amounts of ash emitted from volcanic eruptions that occurred in different periods, reach the marine environment and are stored in the sediment. This study concluded that the Southern Black Sea coasts were under the influence of element enrichment caused by volcanic eruptions in the Meghalian periods. PTE-induced enrichment (for As, Cu, Pb, Zn, Cd, Hg, Ni) in other cores except the EBS-1 core of the Southern Black Sea Region and increases in ecological risks due to this factor were identified based on the examinations performed in the stations located the study area. This increase has emerged as a result of the developments in industrialization and urbanization. Anthropogenic effects were found to be more dominant in the western and central parts of the Southern Black Sea Region. Although the PTE concentrations in the Southern Black Sea sediments show an increasing trend at some points regarding the toxic risk index, they generally do not show significant changes along the core. The difference between these two ecological risk indexes is mainly due to the difference in the parameters addressed in the study. While mPER is based on the enrichment factor of the elements, TRI uses the threshold values specified in the sediment quality guidelines. Another source of enrichment detected in the cores is the volcanic activities that took place in different periods in the past. PTEs originating from volcanic ash accumulate in aquatic ecosystems and are incorporated into biological cycle systems. Parallel to this, PTEs pose a significant threat to the ecological balance even though they come from natural sources. Increasing PTE contamination in the past few years showed that the quality of the Southern Black Sea sediments, exposed to industrialization and urbanization, was deteriorating. For this reason, it is recommended to intervene and take action especially in regards to urban and industrial wastes and to treat these wastes before they reach the marine environment.

Ethical approval

Not applicable.

Funding

This study was supported by the Scientific and Technological Research Council of Türkiye (TUBITAK) within the scope of project Effects of Black Sea sediments and deep waters on biota (Project number: 107Y182). We thank TUBITAK for their support.

CRediT authorship contribution statement

ozkan yesim ebru: Conceptualization, Data curation, Formal analysis, Funding acquisition, Investigation, Methodology, Project administration, Resources, Supervision, Validation, Writing – original draft, Writing – review & editing. **Fural Şakir:** Conceptualization, Data curation, Formal analysis, Methodology, Software, Supervision, Validation, Visualization, Writing – original draft, Writing – review & editing. **Kükrer Serkan:** Conceptualization, Methodology, Supervision, Validation, Writing – original draft, Writing – review & editing.

Declaration of Generative AI and AI-assisted technologies in the writing process

During the preparation of this work the authors used Chatgpt in order to Control of language, expression and punctuation. After using this tool/service, the authors reviewed and edited the content as needed and takes full responsibility for the content of the publication.

Declaration of Competing Interest

The authors declare that they have no known competing financial interests or personal relationships that could have appeared to influence the work reported in this paper.

Data Availability

Data will be made available on request.

Acknowledgements

This study was supported by the Scientific and Technological Research Council of Türkiye (TUBITAK) within the scope of project 114Y419. We thank TUBITAK and Prof. Dr. Hasan Baha Büyükışık for their support.

Consent to participate

Not applicable.

Consent to publish

All authors approve the publication of the article in your journal.

References

Al-Kahtany, K., Nour, E.H., Giacobbe, S., Alharbi, T., El-Sorogy, A.S., 2023a. Heavy metal pollution in surface sediments and human health assessment in southern Al-Khobar coast, Saudi Arabia. Mar. Pollut. Bull. 187 https://doi.org/10.1016/j.marpolbul.2022.114508.

Al-Kahtany, K., Nour, E.H., Giacobbe, S., El-Sorogy, A.S., Alharbi, T., 2023b. Ecological and health risk assessment of heavy metals contamination in mangrove sediments, Red Sea coast. Mar. Pollut. Bull. 192 https://doi.org/10.1016/j.marpolbul.2023.115000.
Alkan, A., Serdar, S., Fidan, D., 2008. Black Sea and pollution. Aquacult. Studies 8, 6–7.
Atıcı, G., Türkecan, A., 2017. Volcanoes of anatolia. Bull. Nat. Resour. Econ. 22, 1–18.
Avcı, Z.U., 2019. Determination of risky ground areas caused by mining activities in Istanbul. Çanakkale Onsekiz Mart Univ. J. Grad. Sch. Nat. Appl. Sci. 5, 293–306. https://doi.org/10.28979/comufbed.581174.
Bakan, G., Büyükgüngör, H., 2000. The Black Sea. Mar. Pollut. Bull. 41, 24–43.
Bakan, G., Özkoç, H.B., 2007. An ecological risk assessment of the impact of heavy metals in surface sediments on biota from the mid-Black Sea coast of Turkey. Int. J. Environ. Stud. 64, 45–57. https://doi.org/10.1080/00207230601125069.
Balık, İ., 2019. Fisheries jurisdiction and fisheries activities in the Black sea coastal countries. Acta Aquat. Turc. 15, 117–125. https://doi.org/10.22392/actaquatr.577155.
Balkıs, N., Topçuoğlu, S., Güven, K.C., Öztürk, B., Topaloğlu, B., Kırbaşoğlu, Ç., et al., 2007. Heavy metals in shallow sediments from the Black Sea, Marmara Sea and Aegean Sea regions of Turkey. J. Black Sea Mediterr. Environ. 13, 147–153.
Bastami, K.D., Neyestani, M.R., Shemirani, F., Soltani, F., Haghparast, S., Akbari, A., 2015. Heavy metal pollution assessment in relation to sediment properties in the coastal sediments of the southern Caspian Sea. Mar. Pollut. Bull. 92, 237–243. https://doi.org/10.1016/j.marpolbul.2014.12.035.
Bat, L., Özkan, E.Y., 2019. Heavy metal levels in sediment of the Turkish Black Sea Coast. In: Pour içinde, K.M. (Ed.), , Oceanography and Coastal Informatics: Breakthroughs in Research and Practice (86-107). Information Resources Management Association, USA. https://doi.org/10.4018/978-1-5225-7308-1.ch004.
Bat, L., Baki, O.G., Karakaş, E., Vişne, A., Okkay, Ç., 2014. Studies using indicator organisms of the Black sea to understand the ecosystem responses of heavy metals. Aquac. Stud. 14, 71–91. https://doi.org/10.17693/yunusae.vi.235399.
Bilhan, Ö., İlalan, F., 2021. Evaluation of arsenic heavy metal in Kizilirmak (Nevşehir-Turkey) river sediments using undisturbed sediment sampler. Eur. J. Sci. Technol. 24, 302–308. https://doi.org/10.31590/ejosat.900690.
Brady, J.P., Ayoko, G.A., Martens, W.N., Goonetilleke, A., 2015. Development of a hybrid pollution index for heavy metals in marine and estuarine sediments. Environ. Monit. Assess. 187 https://doi.org/10.1007/s10661-015-4563-x.
Cheng, K., Tian, H.Z., Zhao, D., Lu, L., Wang, Y., Chen, J., et al., 2013. Atmospheric emission inventory of cadmium from anthropogenic sources. Int. J. Environ. Sci. Technol. 11, 605–616. https://doi.org/10.1007/s13762-013-0206-3.
De Master, D.J., 1981. The supply and accumulation of silica in the marine environment. Geochim. Et. Cosmochim. Acta 45, 1715–1732. https://doi.org/10.1016/0016-7037(81)90006-5.
Elderwish, N.M., Taştan, Y., Sönmez, A.Y., 2019. Seasonal investigation of heavy metal accumulation in waters of western Black Sea Coasts of Turkey. Menba Kastamonu Univer. Faculty Fish. J. 5, 1–8.
Ergin, M., 2020. Investigation of anthropogenic heavy metal pollution in core sediments of Eckernförder and Geltinger bays, West Baltic Sea, Germany. Geol. Bull. Turk. 63, 21–42. https://doi.org/10.25288/tjb.590966.
Ergül, H.A., Topçuoğlu, S., Ölmez, E., Kırbaşoğlu, Ç., 2008. Heavy metals in sinking particles and bottom sediments from the eastern Turkish coast of the Black Sea. Estuar., Coast. Shelf Sci. 78, 396–402. https://doi.org/10.1016/j.ecss.2008.01.006.
Frontalini, F., Coccioni, R., 2007. Benthic foraminifera for heavy metal pollution monitoring: a case study from the central Adriatic Sea coast of Italy. Estuar., Coast. Shelf Sci. 76, 404–417. https://doi.org/10.1016/j.ecss.2007.07.024.
Fural, Ş., Kükrer, S., Cürebal, İ., 2020. Geographical information systems based ecological risk analysis of metal accumulation in sediments of İkizcetepeler Dam Lake (Turkey). Ecol. Indic. 119 https://doi.org/10.1016/j.ecolind.2020.106784.
Fural, Ş., Kükrer, S., Aykır, D., Cürebal, İ., 2022. Ecological degradation and non-carcinogenic health risks of potential toxic elements: a GIS-based spatial analysis for Doganci Dam (Turkey). Environ. Monit. Assess. 194. https://doi.org/10.1007/s10661-022-09870-4.
Gaudette, H.E., Flight, W.R., Toner, L., Folger, W., 1974. An inexpensive titration method for the 451determination of organic carbon in recent sediments. J. Sediment. Petrol. 44, 249–253.
Goulding, I.C., Stobberup, K.A., Higgins, T.O., 2014. Potential economic impacts of achieving good environmental status in Black Sea fisheries. Ecol. Soc. 19 https://www.jstor.org/stable/26269641.
Güler, I., Yüksel, Y., Yalçıner, A.C., Ünal, A., Yerli, U., Çevik, E., et al. , 2004. Istanbul Strait current measurements and initial data. Turkey's Coastal and Marine Areas V. National Conference Full Text Proceedings. 797–804, Adana.
Hakanson, L., 1980. An ecological risk index for aquatic pollution control: a sedimentological approach. Water Res. (8), 975–1001. https://doi.org/10.1016/0043-1354(80)90143-8.
Homens, M.M., Blum, J., Canario, J., Caetano, M., Costa, A.M., Lebreiro, S.M., et al., 2013. Tracing anthropogenic Hg and Pb input using stable Hg and Pb isotope ratios in sediments of the central Portuguese Margin. Chem. Geol. 336, 62–71. https://doi.org/10.1016/j.chemgeo.2012.02.018.
Järup, L., 2003. Hazards of heavy metal contamination. Br. Med. Bull. 68, 167–182. https://doi.org/10.1093/bmb/ldg032.
Jeddi, K., Fatnassi, M., Chaieb, M., Siddique, K.H., 2021. Tree species as a biomonitor of metal pollution in arid Mediterranean environments: case for arid southern Tunisia. Environ. Sci. Pollut. Res. 28, 28598–28605. https://doi.org/10.1007/s11356-021-12788-y.
Jitar, O., Teodosiu, C., Oros, A., Plavan, G., Nicoara, M., 2015. Bioaccumulation of heavy metals in marine organisms from the Romanian sector of the Black Sea. N. Biotechnol. 32, 369–378. https://doi.org/10.1016/j.nbt.2014.11.004.
Joksimović, D., Perošević, A., Castelli, A., Pestorić, B., Šuković, D., Đurović, D., 2020. Assessment of heavy metal pollution in surface sediments of the Montenegrin coast: a 10-year review. J. Soils Sediment. 20, 2598–2607. https://doi.org/10.1007/s11368-019-02480-7.
Kalkan, S., 2022. Heavy metal resistance of marine bacteria on the sediments of the Black Sea. Mar. Pollut. Bull. 179 https://doi.org/10.1016/j.marpolbul.2022.113652.
Kazancı, N., 2018. Stages of the Holocene. Geol. Bull. Turk. 61, 359–361. https://doi.org/10.25288/tjb.460471.
Kükrer, S., Erginal, A.E., Kılıç, Ş., Bay, Ö., Akarsu, T., Öztura, E., 2020. Ecological risk assesment of surface sediments of Çardak Lagoon along a human disturbance gradient. Environ. Monit. Asses. 192. https://doi.org/10.1007/s10661-020-08336-9.
Lebedev, L.A., Chernyshev, I.V., Chugaev, A.V., Gol'tsman, Y.V., Bairova, E.D., 2010. Geochronology of eruptions and parental magma sources of Elbrus volcano, the Greater Caucasus: K-Ar and Sr-Nd-Pb isotope data. Geochem. Int. 48, 41–67. https://doi.org/10.1134/S0016702910010039.
Lorenzen, C., 1971. Chlorophyll-degradation products in sediments of Black Sea. Woods Hole Oceanogr. Inst. Contrib. 28, 426–428.
Mac Donald, D.D., Ingersoll, C.G., Berger, T.A., 2000. Development and evaluation of consensus-based sediment quality guidelines for freshwater ecosystems. Arch. Environ. Contam. Toxicol. 39, 20–31. https://doi.org/10.1007/s002440010075.
Makedonski, L., Peycheva, K., Stancheva, M., 2017. Determination of heavy metals in selected black sea fish species. Food Control 72, 313–318. https://doi.org/10.1016/j.foodcont.2015.08.024.
Mineral Research and Exploration Department (MTA), (2021). http:// earth sciences. mta.gov.tr/mainpage.aspx.
Nour, E.H., El-Sorogy, S.A., El-Wahab, M.A., Nouh, E.S., Mohamaden, M., Al-Kahtany, K., 2019. Contamination and ecological risk assessment of heavy metals pollution from the Shalateen coastal sediments, Red Sea, Egypt. Mar. Pollut. Bull. 144, 167–172. https://doi.org/10.1016/j.marpolbul.2019.04.056.
Nour, E.H., Alshehri, F., Sahour, H., El-Sorogy, A.S., 2022. Evaluation of sediment and water quality of Ismailia Canal for heavy metal contamination, Eastern Nile Delta, Egypt. Reg. Stud. Mar. Sci. 56, 102714 https://doi.org/10.1016/j.rsma.2022.102714.
Özkan, E.Y., Fural, Ş., Kükrer, S., Büyükışık, H.B., 2022. Seasonal and spatial variations of ecological risk from potential toxic elements in the southern littoral zone of İzmir Inner Gulf, Turkey. Environ. Sci. Pollut. Res. 29, 62669–62689. https://doi.org/10.1007/s11356-022-19987-1.
Özkoç, H.B., Arıman, S., 2022. Contamination and risk assessment of heavy metals in coastal sediments from the Mid-Black Sea, Turkey. Stoch. Environ. Res. Risk Assess. https://doi.org/10.1007/s00477-022-02300-4.
Özşeker, K., Erüz, Ç., Terzi, Y., 2022. Spatial distribution and ecological risk evaluation of toxic metals in the southern Black Sea coastal sediments. Mar. Pollut. Bull. 182 https://doi.org/10.1016/j.marpolbul.2022.114020.
Öztürk, İ., Şeker, M., 2021. Ecology of the Sea of Marmara. Mucilage Formation, Interaction and Solution Proposals. Ankara: Turkish Academy of Sciences.,.
Peng, Z., Guo, Z., Wang, Z., Zhang, R., Wu, Q., Gao, H., et al., 2022. Species-specific bioaccumulation and health risk assessment of heavy metal in seaweeds in tropic coasts of South China Sea. Sci. Total Environ. 832 https://doi.org/10.1016/j.scitotenv.2022.155031.
Rai, K.P., 2008. Heavy metal pollution in aquatic ecosystems and its phytoremediation using wetland plants: an ecosustainable approach. Int. J. Phytoremediat. 10, 133–160. https://doi.org/10.1080/15226510801913918.
Russel, R.J., 1954. Alluvial morphology of Anatolian rivers. Ann. Assoc. Am. Geogr. 44, 363–391.
Sanei, H., Outridge, M., Oguri, K., Stern, G.A., Thamdurp, B., Wenzhöfer, F., Wang, F., Glud, N.R., 2021. High mercury accumulation in deep-ocean hadal sediments. Sci. Rep. https://doi.org/10.1038/s41598-021-90459-1.
Schlichting, E., Blume, H. , 1966. Bodenkundliches praktikum. Hamburg und Berlin: Verlag Paul.
Surricchio, G., Pompilio, L., Novelli, A.A., Scamosci, E., Marinangeli, L., Tonucci, L., et al., 2019. Evaluation of heavy metals background in the Adriatic Sea sediments of Abruzzo region, Italy. Sci. Total Environ. 684, 445–457. https://doi.org/10.1016/j.scitotenv.2019.05.350.
Sutherland, R., 2000. Bed sediment associated trace metals in an urban stream, Oahu. Hawaii. Environ. Geol. 39, 611–627.
Topçuoğlu, S., Güven, K.C., Balkıs, N., Kırbaşoğlu, Ç., 2003. Heavy metal monitoring of marine algae from the Turkish Coast of the Black Sea, 1998–2000. Chemosphere 52, 1683–1688. https://doi.org/10.1016/S0045-6535(03)00301-1.
Ustaoğlu, F., Islam, M.S., 2020. Potential toxic elements in sediment of some rivers at Giresun, Northeast Turkey: a preliminary assessment for ecotoxicological status and health risk. Ecol. Indic. 113, 1–14. https://doi.org/10.1016/j.ecolind.2020.106237.
Ustaoğlu, F., Tepe, Y., 2019. Water quality and sediment contamination assessment of Pazarsuyu Stream, Turkey using multivariate statistical methods and pollution indicators. International Soil and Water Conservation. Research 7, 47–56.
Varol, M., Ustaoğlu, F., Tokatlı, C., 2022. Ecological risk assessment of metals in sediments from three stagnant water bodies in Nothern Turkey. Curr. Pollut. Rep. 61, 1–13. https://doi.org/10.1007/s40726-022-00239-2.
Vera, S., Dmitrii, B., Artem, L., Larisa, K., 2020. Assessing the pollution level in the kuban river basin by multivariate cluster analysis. Asian J. Water Environ. Pollut. 17, 73–80.
Xie, S., Jiang, W., Sun, J., Yu, K., Feng, C., Han, Y., et al., 2022. Interannual variation and sources identification of heavy metals in seawater near shipping lanes: Evidence from a coral record from the northern South China Sea. Sci. Total Environ. 854 https://doi.org/10.1016/j.scitotenv.2022.158755.

Xu, Xiaoda, Cao, Zhimin, Zhang, Zhixun, Li, Rihui, Hu, Bangqi, 2016. Spatial distribution and pollution assessment of heavy metals in the surface sediments of the Bohai and Yellow Seas. Mar. Pollut. Bull. 110, 596–602. https://doi.org/10.1016/j.marpolbul.2016.05.079.

Yanagi, T., 1990. Currents and sediment transport in the Seto Inland sea. Jpn. Residual Curr. Long. Term. Transp. 38, 348–355.

Yılmaz, T., Alp, İ., Deveci, H., Duran, C., Oktay, C., 2007. Ferric sulfate leaching of Kayabaşı massive copper ore. Istanb. Univ. Fac. Eng. J. Earth Sci. 20, 63–69.

Yücesoy, F., Ergin, M., 1992. Heavy-metal geochemistry of surface sediments from the southern Black Sea shelf and upper slope. Chem. Geol. 99, 265–287.

Yüksel, B., Ustaoğlu, F., Tokatlı, C., Islam, M.S., 2022. Ecotoxicological risk assessment for sediments of Çavuşlu stream in Giresun, Turkey: association between garbage disposal facility and metallic accumulation. Environ. Sci. Pollut. Res. 29, 17223–17240. https://doi.org/10.1007/s11356-021-17023-2.

Zhang, G., Bai, J., Zhao, Q., et al., 2016. Heavy metals in wetland soils along a wetland-forming chronosequence in the Yellow River Delta of China: levels, sources and toxic risks. Ecol. Indic. 69, 331–339 https://doi.org/1010.1016/j.ecolind.2016.04.042.

Zhang, L., Ye, X., Feng, H., Jing, Y., Ouyang, T., Yu, X., 2007. Heavy metal contamination in western Xiamen Bay sediments and its vicinity, China. Mar. Pollut. Bull. 54, 974–982.